Journal of the Korean Physical Society, Vol. 46, June 2005, pp. S214∼S217

Electroreflectance Study of $Zn_{0.8}Mg_{0.2}O$/ZnO Nanorod Heterostructures

Sung Soo Kim, Hyun Jin Lim and Hyeonsik Cheong*
Department of Physics, Sogang University, Seoul 121-742

Won Il Park and Gyu-Chul Yi
Department of Materials Science and Engineering, Pohang University of Sceince and Technology, Pohang 790-784

(Received 18 August 2004)

ZnO, due to its large exciton binding energy which enables excitonic recombination at room temperature, is attracting much attention as a material for room-temperature UV devices. In particular, ZnO nanorod has attracted a great deal of attention because of the commercial interest in short-wavelength semiconductor laser diodes and nanometer-scale electronic devices. $Zn_{0.8}Mg_{0.2}O$/ZnO nanorod heterostructures were grown by metal-organic vapor-phase epitaxy on catalyst-free ZnO nanorods. Electroreflectance measurements were carried out at temperatures between 90 K and 295 K and compared with photoluminescence data. Quantum confinement effects in $Zn_{0.8}Mg_{0.2}O$/ZnO nanorod heterostructures were observed.

PACS numbers: 78.67.Bf, 78.20.Jq, 73.21.Fg
Keywords: Zinc oxide, Nanorod, Heterostructure, Electroreflectance

I. INTRODUCTION

ZnO, a wide-bandgap semiconductor with a bandgap energy of about 3.4 eV, is attracting much interest due to its large exciton binding energy and high bond strength, which are advantageous for optoelectronic applications such as light emitters and ultraviolet photodetectors [1–3]. Successful fabrication of ZnO-based nanorods or nanowires by using metal-organic vapor-phase epitaxy (MOVPE) [4] has raised the prospect of utilizing this material in nano-sized optoelectronic devices [5]. In order to control the device characteristics, bandgap engineering through fabrication of heterostructures is desirable. Since alloying MgO into ZnO increases the bandgap energy, one can vary the heterostructure bandgap energy of multiple quantum wells (MQW's) or superlattices of ZnO and $Zn_{1-x}Mg_xO$ by adjusting the thickness of each layer. It is known that the photoluminescence (PL) energy is increased to about 4 eV by alloying Mg into this material: as the Mg concentration x in $Zn_{1-x}Mg_xO$ increases from 0 to 0.5, the PL energy increases from 3.35 to 4.05 eV [6]. These results were confirmed by spectroscopic ellipsometry measurements [7]. Recently, multiple quantum wells of $Zn_{1-x}Mg_xO$/ZnO have been successfully grown on high-quality ZnO nanorods by using MOVPE, and PL measurements were used to demonstrate quantum confinement effects [8]. However, since PL measurements probe only the lowest-energy radiative recombination, it is difficult to pinpoint the bandgap energy. Furthermore, PL is incapable of probing higher-energy transitions, which may play a major role in determining the device properties.

An alternative method of determining the bandgap energies is electroreflectance. In this technique, an ac electric field is applied to the sample and the modulation in the reflectance due to the electric field is spectroscopically measured to obtain derivative-like spectra. Since this technique directly probes the joint density of states of the material being studied, the existence of impurity levels or nonradiative recombination centers hardly affects the spectra. Furthermore, unlike PL, it can be used to determine with high accuracy the critical point energies at room temperature. However, usual electroreflectance (ER) measurements cannot be performed on nanorod samples, because fabricating electrodes on nanorods is impracticable. We therefore used the contactless electroreflectance method pioneered by Pollak and coworkers [9]. Since no contact electrode is needed, the technique can be easily applied to nanorod samples. In this paper, we report on the results of ER measurements on $Zn_{0.8}Mg_{0.2}O$/ZnO nanorod heterostructures.

II. EXPERIMENT

We used metal-organic vapor-phase epitaxy (MOVPE) to grow high-quality ZnO nanorods, thus eliminating

*E-mail: hcheong@sogang.ac.kr

the metal catalyst usually required in other methods. To fabricate heterostructures within the nanorods, $Zn_{1-x}Mg_xO$ ($x \approx 0.2$) alloy was employed as the barrier material, since it has a lattice mismatch with ZnO of less than 1 %. ZnO nanorods were first prepared on $Al_2O_3(00 \cdot 1)$ substrates by using MOVPE. Nanorods are formed as a result of preferential growth along the *c*-axis of ZnO, offering an ideal method for fabrication of nanoscale heterostructures. By introducing Mg precursor into the reactor, $Zn_{1-x}Mg_xO$ layers were epitaxially grown only on the tips of the ZnO nanorods. The MQW nanorods prepared in this study consist of 10 periods of $Zn_{0.8}Mg_{0.2}O$/ZnO on ZnO nanorods (a schematic diagram of the MQW nanorods is shown in Figure 1). For ZnO nanorod growth, we employed diethylzinc (DEZn) and oxygen as the reactants with argon as the carrier gas. For $Zn_{1-x}Mg_xO$ growth, bis(cyclopentadienyl)magnesium (Cp2Mg) was used as the Mg precursor, with composition controlled through the partial pressure. The nanorods consist of 10 periods of 4.5-nm ZnO/6.0-nm $Zn_{1-x}Mg_xO$, as confirmed by transmission electron microscopy (TEM). The composition of the $Zn_{1-x}Mg_xO$ layers was determined by energy dispersive X-ray spectroscopy, and for this sample x was approximately 0.2. The details of sample growth and structural characterization have been reported elsewhere [8].

Contactless electroreflectance measurements were taken at temperatures between 90 K and room temperature by using a square wave of 800 V at 1 kHz as the modulation potential. A 100-W xenon arc lamp combined with a Spex 270M monochromator with a 2400-grooves/mm grating was the light source. The sample was placed in a flow-type cryostat with liquid nitrogen as the cryogen. A low-noise UV-grade silicon photodiode was used as the detector. The signal from the detector was amplified by a current preamplifier and the dc and ac components of the signal were recovered by a digital voltmeter and a lock-in amplifier, respectively [10].

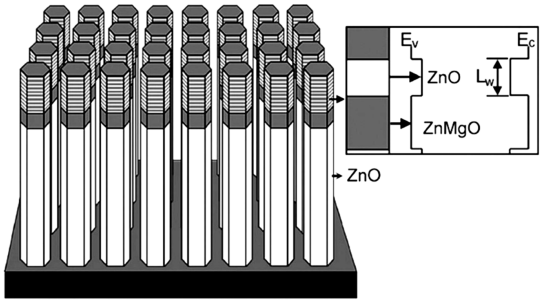

Fig. 1. Schematic of 4.5-nm ZnO/6.0-nm $Zn_{1-x}Mg_xO$ MQW nanorods. $Zn_{1-x}Mg_xO$ has higher bandgap energy and forms the barriers.

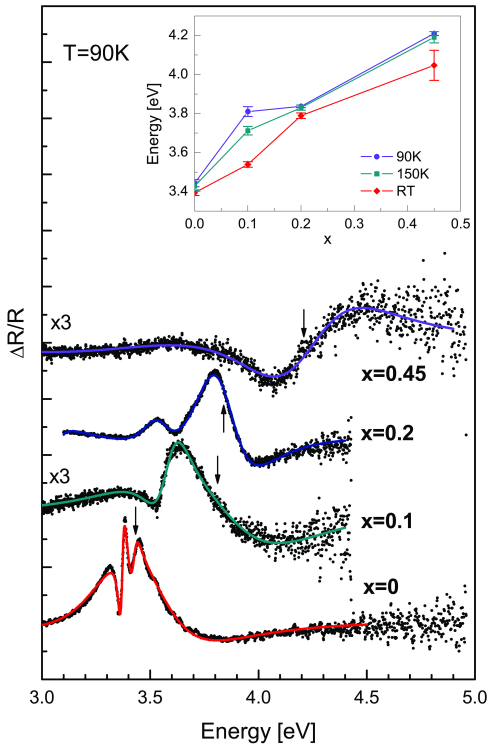

Fig. 2. ER spectra of $Zn_{1-x}Mg_xO$ thin films, taken at 90 K. The continuous curves are fits to the data by using Eq. (1). The inset shows the bandgap energy as a function of x.

III. RESULTS AND DISCUSSION

In order to establish the dependence of the bandgap energy on the Mg concentration, ER measurements were performed on $Zn_{1-x}Mg_xO$ thin films for various x values. Figure 2 shows the ER spectra of $Zn_{1-x}Mg_xO$ thin films taken at 90 K. Derivative-like features, characteristic of bandgaps, are seen. In order to extract the exact value of the bandgap energy from the spectra, the measured data are compared with a theoretical lineshape function by using the low-field approximation [9]. In this limit, the modulated reflectance ratio is given by

$$\frac{\Delta R}{R} = A \times \mathrm{Re}[e^{i\phi}(E - E_g + i\Gamma)^{-m}], \qquad (1)$$

where E_g is the bandgap energy, Γ a broadening parameter, m a dimensionality parameter, ϕ a phase factor, and A the amplitude. The measured spectra can be fitted to Eq. (1) by using E_g, Γ, m, ϕ, and A as the fitting parameters. When multiple critical points are involved, a linear combination of Eq. (1) is used to account for different contributions. The inset shows the bandgap energy thus determined as a function of x. A monotonic dependence of the bandgap on x is seen. The multiple-peak structure below the bandgap seen in the ER spectrum for $x = 0$ is exciton-related. Note that the bandgap energies are consistently higher than the PL peak energies reported earlier [8]. This is reasonable because the PL peak usually occurs at the lowest-energy transition, in this case the lowest-energy exciton transition, whereas ER probes

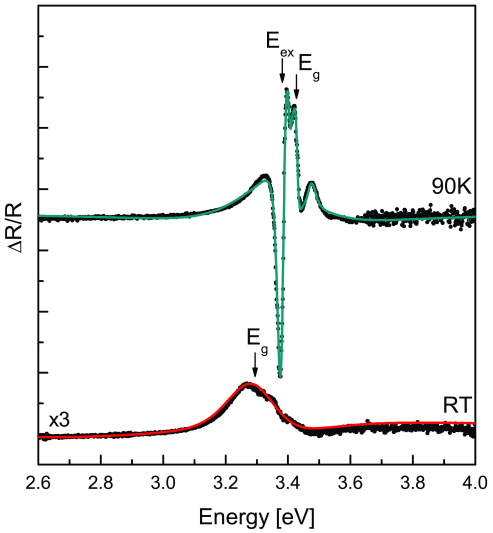

Fig. 3. ER spectra of a ZnO nanorod sample, taken at room temperature and at 90 K. The continuous curves are fits to the data.

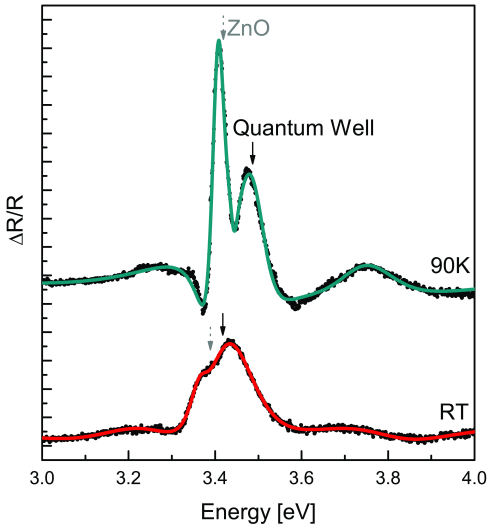

Fig. 4. ER spectra of a 4.5-nm ZnO/6.0-nm $Zn_{0.8}Mg_{0.2}O$ nanorod-heterostructure sample, taken at room temperature and at 90 K. The continuous curves are fits to the data..

both the exciton transitions and the band-to-band transitions.

Figure 3 shows the ER spectra of ZnO nanorods taken at room temperature and at 90 K. The bandgap energy of 3.42 $\pm$ 0.01 eV at 90 K is within the error bars of that of ZnO thin film (3.40 $\pm$ 0.02 eV) at 90 K. Quantum confinement effect is not expected, since the diameter of the nanorods is approximately 40 nm, too large for any appreciable confinement effect. The exciton-related below-bandgap structures are more pronounced than for the thin-film sample, presumably indicating a higher crystal quality.

Figure 4 shows the ER spectra of $Zn_{0.8}Mg_{0.2}O$/ZnO nanorod heterostructures at room temperature and at 90 K. In addition to the ZnO and $Zn_{0.8}Mg_{0.2}O$ features, there is a well-resolved spectral feature at 3.48 $\pm$ 0.01 eV, between the bandgaps of ZnO and $Zn_{0.8}Mg_{0.2}O$. This is interpreted as being due to the quantum-confined states in MQW. This transition is blue-shifted relative to that of ZnO nanorods, due to the quantum confinement. Transitions between higher-energy quantum-well states are not resolved, although there should be more than one confined level each in the conduction and the valence band. Inhomogeneous broadening due to small fluctuations in the well and barrier widths would significantly reduce the ER signal. In this regard, a single-quantum-well sample may be more advantageous in studying the higher-energy confined levels. In order to establish a correlation between the transition energy and the MQW parameters, such as the well width and the barrier width, more study is needed.

IV. SUMMARY

Contactless electroreflectance measurements were carried out on ZnO and $Zn_{1-x}Mg_xO$ thin films, ZnO nanorods, and ZnO/$Zn_{1-x}Mg_xO$ nanorod heterostructures at temperatures between room temperature and 90 K. The ER spectrum of the nanorod-heterostructure sample shows indications of quantum confinement effects. More study is needed to quantify the correlation between the structural parameters and the quantum confinement effects.

ACKNOWLEDGMENTS

This work was supported by KOSEF through the Quantum Photonic Science Research Center at Hanyang University and by MOST through the National R&D Project for Nano Science.

REFERENCES

[1] D. M. Bagnall, Y. F. Chen, Z. Zhu, T. Yao, S. Koyama, M. Y. Shen and T. Goto, Appl. Phys. Lett. **70**, 2230 (1997).
[2] Z. K. Tang, G. K. Wong, P. Yu, M. Kawasaki, A. Ohtomo, H. Koinuma and Y. Segawa, Appl. Phys. Lett. **72**, 3270 (1997).
[3] W. I. Park, S.-J. An, G.-C. Yi and H. M. Jang, J. Mater. Res. **16**, 1358 (2001).
[4] W. I. Park, D. H. Kim, S.-W. Jung and G.-C. Yi, Appl. Phys. Lett. **80**, 4232 (2002).
[5] M. S. Gudiksen, L. J. Lauhon, J. Wang, D. C. Smith and C. M. Lieber, Nature **415**, 617 (2002).

[6] W. I. Park, G.-C. Yi and H. M. Jang, Appl. Phys. Lett. **79**, 2022 (2001).
[7] T. D. Kang, H. Lee, W. I. Park and G.-C. Yi, J. Korean Phys. Soc. **44**, 129 (2004).
[8] W. I. Park, G.-C. Yi, M. Kim and S. J. Pennycook, Adv. Mater. **15** 526 (2003).
[9] F. H. Pollak and H. Shen, Mater. Sci. Eng. R **10**, 275 (1993).
[10] S. S. Kim, H. Cheong, J. D. Song, Y. M. Park, J. C. Shin, Y. J. Park, W. J. Choi and J. I. Lee, J. Korean Phys. Soc. **45**, 145 (2004).